https://doi.org/10.14669/AM/225585

MODERN SOLUTIONS FOR REDUCING THE AERODYNAMIC DRAG OF PASSENGER CARS

ŁUKASZ OKRUCH[1], WIESŁAW ZALEWSKI[2], MATEUSZ MIKOŁAJCZAK[3], MAREK MILLER[4]

Abstract

The paper presents three groups of aerodynamic solutions that are currently common in the bodies of passenger cars from various manufacturers. Solutions of this type should reduce aerodynamic drag, which allows for lower electricity or fuel consumption. This also translates into increased vehicle range and compliance with stringent emission standards. Such solutions also play an important aesthetic role, increasing the visual appeal of the car body for the customer. The research was performed using the geometry of an SUV passenger car body as a reference point. This is currently one of the most popular car body types in Europe. The car body was configured to meet the requirements of an electric vehicle. The main difference from its combustion engine counterpart was the use of a flat floor. The base body was modified by adding various aerodynamic elements to the front and rear of the vehicle. They also changed the airflow of the base body in the area of the vehicle floor. The aerodynamic drag forces of the base geometry and its modified variants were determined using advanced computational fluid dynamics tools. The Ansys Fluent computational package was used in the analyses. The solutions used, computational models and results obtained are presented. The calculations confirmed the significant impact of the tested solutions on the aerodynamics of the car. After numerical analysis, the most promising solutions were selected and incorporated into the base geometry. Models were then prepared for testing in a wind tunnel, and tests were conducted which confirmed the results obtained in the numerical analyses. The reduction in aerodynamic drag achieved was approximately 9%. Based on the tests performed, it was concluded that additional airflow control solutions applied locally to the car body can effectively reduce its aerodynamic drag.

[1] Research Group for New Automotive Technologies, Łukasiewicz Research Network – Automotive Industry Institute, Warsaw, Poland, email: lukasz.okruch@pimot.lukasiewicz.gov.pl, ORCID: 0000-0001-7129-135X

[2] Aerodynamics Department, CFD section, Łukasiewicz Research Network – Institute of Aviation, Warsaw, Poland, email: Wieslaw.Zalewski@ilot.lukasiewicz.gov.pl, ORCID: 0000-0002-2983-272X

[3] Research Group for New Automotive Technologies, Łukasiewicz Research Network – Automotive Industry Institute, Warsaw, Poland, email: mateusz.mikolajczak@pimot.lukasiewicz.gov.pl, ORCID: 0009-0001-6580-4144

[4] Aerodynamics Department, Aerodynamics Research Laboratory, Łukasiewicz Research Network – Institute of Aviation, Warsaw, Poland, email: marek.miller@ilot.lukasiewicz.gov.pl, ORCID: 0000-0002-1328-6541

Keywords: aerodynamic drag reduction; SUV car body, electric vehicle; Computational Fluid Dynamics; vehicle aerodynamics

1. Introduction

In the early years of automotive development, between 1920 and 1945, vehicle drag was a secondary consideration. This was due to low driving speeds and the fact that designers focused their efforts on practical aspects and vehicle production technology. The drag coefficient CD ranged from 0.8 to 0.5. Between 1950 and 1973, we see a marked improvement and increase in the importance of vehicle aerodynamics. The drag coefficient CD of vehicles from that period ranged from 0.5 to 0.4. It was only the outbreak of the fuel crisis in 1973 that changed priorities. Manufacturers in Europe began to develop vehicles with low aerodynamic drag. Over the next 30 years of development, the drag coefficient was reduced to 0.3. According to manufacturers, typical passenger cars currently in production have drag coefficients in the range of 0.22–0.3. The lower range of these values is found among electric vehicles [1, 2, 3]. History of drag coefficient CD of passenger cars is presented in Figure 1.

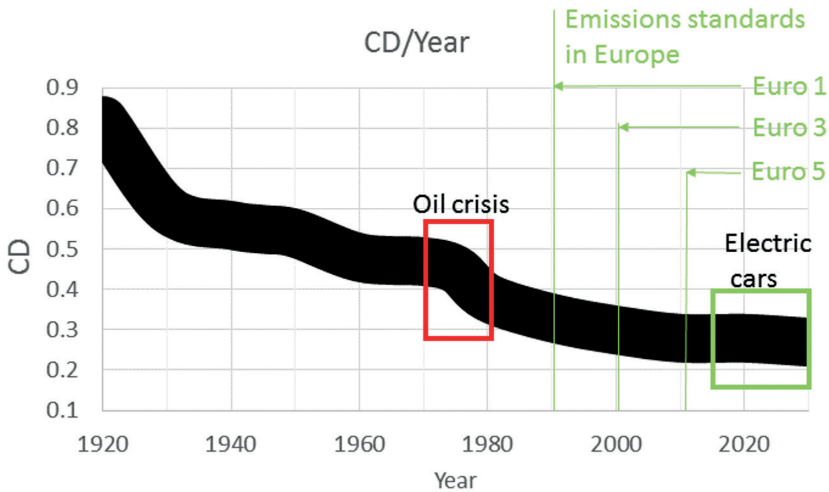

Fig. 1. History of drag coefficient CD of passenger cars [1, 2, 3]

For an average C-segment passenger car traveling on a paved road under standard atmospheric conditions at sea level (in accordance with the International Standard Atmosphere) at low speeds, the main component of resistance is the rolling resistance of the vehicle. Only

https://doi.org/10.14669/AM/225585

at speeds of around 60 km/h the forces of rolling resistance and aerodynamic drag reach similar values. Above 60 km/h, aerodynamic drag dominates. At a speed of 90 km/h, the drag force is already more than twice as high as the rolling resistance. At a speed of 120 km/h, the aerodynamic resistance force is more than four times greater than the rolling resistance [1, 4]. In the analyses presented in this paper, comparative calculations were performed assuming a driving speed of 120 km/h as the typical speed on expressways. Rolling and drag resistance relationship is presented in Figure 2.

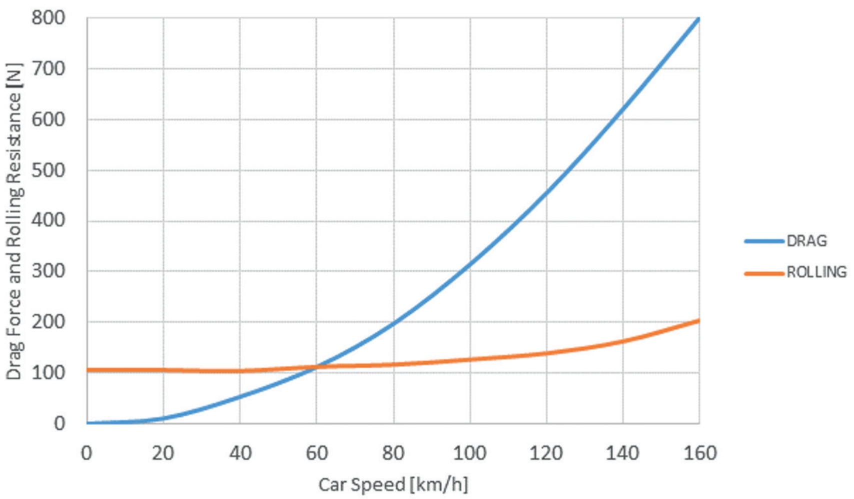

Fig. 2. Rolling and drag resistance [1, 4]

With the development of numerical calculation methods, more and more work in the field of vehicle aerodynamics is being done on computers. Wind tunnels have begun to be used mainly as a form of final validation of numerical results. This significantly speeds up the process of improving vehicle aerodynamics. Additionally, due to the cost of testing in large wind tunnels, only the largest manufacturers and large design offices can afford to conduct such tests. Numerical calculations of vehicle aerodynamics still encounter significant problems and limitations. The main factors that generate problems in computational vehicle aerodynamics are:

- unstreamlined shapes and bluff bodies, generating large flow separation zones,
- low aspect ratio, requiring 3D calculations,
- interaction between individual parts of the vehicle body,
- strong interaction with the ground surface,
- laminar and turbulent flow zones,
- complex geometry created by continuous and discontinuous surfaces.

https://doi.org/10.14669/AM/225585

The literature contains a number of publications describing current computational work on vehicle aerodynamics research. These are studies presenting numerical research on simple vehicle shapes and elements that improve their aerodynamics. Many of them are supported by experimental research.

The paper [4] presents the results of a CFD analysis of three modifications of the rear spoiler and its impact on the flow around the hatchback tailgate. The modifications were carried out on the geometry of an actual Skoda Fabia 3 car. The high level of complexity of the model geometry is noteworthy. The paper does not provide details on CFD modelling, only the final results. Optimizing the design of the rear spoiler resulted in a 2% reduction in the drag coefficient compared to the production version of the car.

Paper [5] presents an analysis of the impact of the basic geometric parameters of a car model on its aerodynamic drag. A parametric model of a highly simplified vehicle body was developed. Optimization calculations were performed. Recommendations for selecting the geometry of the car body's main components are presented. Due to the extremely simplified geometric model, the recommendations presented seem completely out of step with the level of refinement found in modern vehicles.

The paper [6] presents numerical analyses of the use of innovative side spoilers as accessories for the body of a Honda CR-X sports car. Numerical calculations were performed using the RANS method with the k-w sst turbulence model in the Ansys Fluent computational package. The results were not verified experimentally. The article confirms a certain trend observed in numerical simulations of automobiles. When analysing the effect of additional components such as spoilers or wings, the k-w sst turbulence model (typically used in aeronautics) is more commonly employed. In analyses related to the shape of the vehicle body, however, the k-epsilon turbulence model tends to dominate.

Work [7] presents aerodynamic studies of the Lamborghini Aventador sports car. CFD analyses and wind tunnel tests were conducted. By modifying the geometry of the car's rear wing, a reduction in aerodynamic drag of as much as 8% was achieved. However, the tests and simulations were conducted only on a small-scale model without maintaining flow similarity conditions to the real vehicle.

The k-epsilon turbulence model is often recommended in the literature [8].

The analysis of the flow near the rear vehicle body part and interaction with the ground is a frequent topic of research. This solution is crucial in sports cars, but similar elements of vehicle body design are now also appearing in commercial vehicles.

Study [9] presents an analysis that combines the optimization of a car body's geometry with passive methods for controlling flow separation using vortex generators. The study

https://doi.org/10.14669/AM/225585

examined how the position and shape of the vortex generators affect the vehicle's drag. Numerical simulations were performed on a simplified car geometry model (Ahmed body), which is often used to validate CFD methods. A high level of aerodynamic drag reduction (over 10%) was achieved. However, the degree of geometric simplification raises doubts as to whether the obtained results have any relevance to the aerodynamics of modern cars.

The paper [10] presents the development of several aerodynamic packages designed to increase down-force on a Porsche 911. The package consisted mainly of a rear wing and a diffuser. The results obtained from CFD simulations were partially verified using a small-scale model tested in a wind tunnel. Realistic vehicle geometry was used.

Due to the greater freedom in shaping the floor of electric vehicles, there is a strong trend towards adapting similar solutions in electric commercial vehicles. This element was also used in the solutions presented in the paper. Equally interesting are studies on the impact of modifying the geometry of the front part of vehicles. Article [11] presents the results of experimental studies of truck models in a wind tunnel. Through relatively minor modifications, it was possible to reduce aerodynamic drag by 13%.

The paper [12] presents experimental and computational studies of a student formula sports car. This is a very popular class of vehicles among young engineers. Numerous international competitions between rival teams are organised. The paper describes numerical calculations performed using the STAR-CCM package and a comparison with experimental results. The results obtained indicate a good correlation between numerical calculations and experimental tests. The differences obtained did not exceed 4%. The relatively good agreement between numerical models and experimental results allows the use of various automated shape optimisation methods to develop low-drag vehicle geometries. An example of such analyses is the work [13], where the response surface method and a genetic algorithm were used to generate an optimised geometry for minimum aerodynamic drag. The RANS method and the kw-sst turbulence model were used in the numerical calculations. The Ansys Fluent computational package was used. A 26% improvement in aerodynamic drag coefficient was achieved. However, it should be noted that the level of drag reduction depends on the base geometry adopted, and the shape obtained had little in common with commercial vehicles.

A significant number of studies deal with passive flow control issues through the use of various types of vortex generators to control the effect of boundary layer separation in the flow. These solutions provide a reduction in drag force of 2–4% [14, 15] and are not currently used in commercial vehicles.

The literature review cited describes research methods and trends in development found primarily in academic centres specializing in vehicle aerodynamics. It is noteworthy that there are very few available publications from research centres associated with the modern automotive industry or descriptions of work carried out directly for the benefit of that

https://doi.org/10.14669/AM/225585

industry. This is likely due to the fact that such research for major automobile manufacturers is conducted by specialized commercial firms, which do not publish their research results. It appears that academic centres focus on improving the airflow over the upper parts of the car body, while car manufacturers are currently improving the flow in the lower part of the vehicle. This is particularly important for electric cars entering the market. The research presented in this publication focuses precisely on this group of automotive aerodynamic solutions that are and will be present in new electric car models.

2. Description of research, models and methods

It is estimated that in a typical sedan or hatchback car body, the upper part of the body generates 45% of the drag, the lower part of the body approximately 25%, and the wheels and wheel arches approximately 30% [2]. The modifications described in the study concerned the front, floor and rear sections. It therefore seems that there is theoretically significant potential for reducing drag, provided that effective solutions are implemented.

For comparative calculations, a base geometry modelled on a passenger car with an SUV body was prepared. These types of cars currently dominate the European market. Below in Figure 3 are examples of the ElectroMobility Poland Izera [16] and Volkswagen ID 4 [17] electric cars. These are modern electric cars, prototypes of which appeared in 2020. Only the ID 4 has entered the market.

(a) **(b)**

Fig. 3. Electric cars: (a), (b) Izera ID 4 [16, 17]

Figure 4 shows the basic geometry to which various elements affecting the aerodynamics of the vehicle were added as part of the proposed modifications.

https://doi.org/10.14669/AM/225585

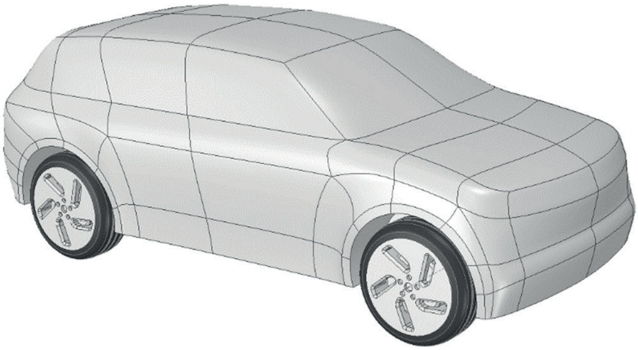

Fig. 4. Base geometry in general view [Created by the authors]

The proposed modifications to the base geometry are presented below. They have been divided into three groups. All the solutions presented in each group were the result of a series of preliminary numerical simulations and yielded the most promising results. The first group, marked WT, included air ducts blowing air onto the front wheel. This solution is currently very common in passenger cars. Three variants of the ducts shown in the figure below were analysed. All numerical simulations and wind tunnel tests were carried out for a car body with wheels. The wheels have been omitted from some of the drawings only for clarity. The geometries of the WT group are shown in the Figures 5–8.

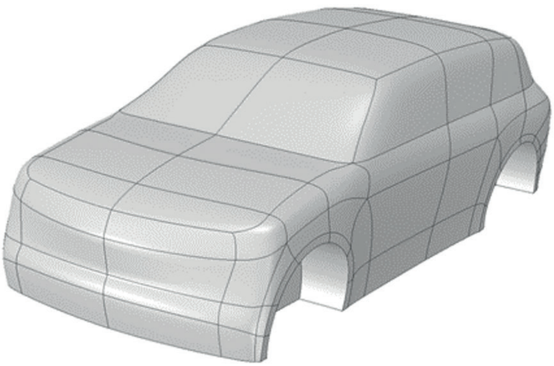

Fig. 5. Base geometry with view of the front bumper [Created by the authors]

https://doi.org/10.14669/AM/225585

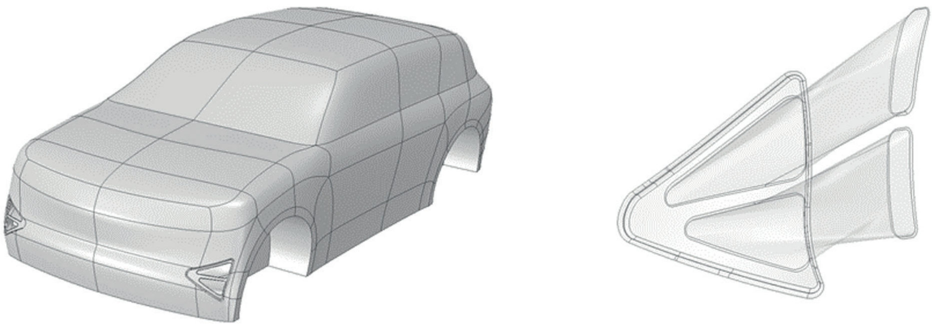

Fig. 6. WT_v1 modification and flow duct details [Created by the authors]

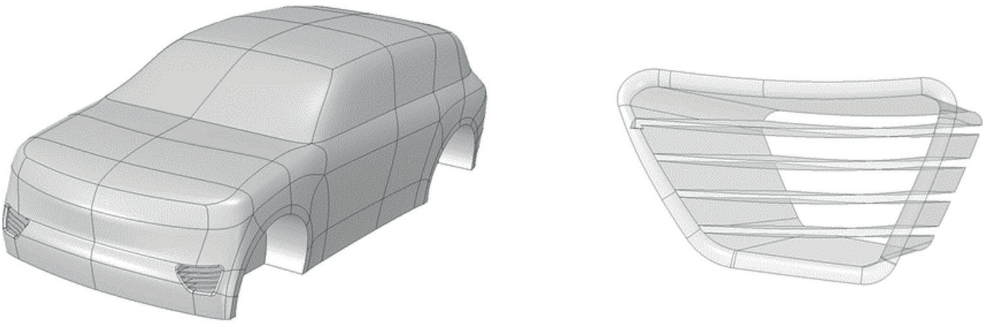

Fig. 7. WT_v2 modification and flow duct details [Created by the authors]

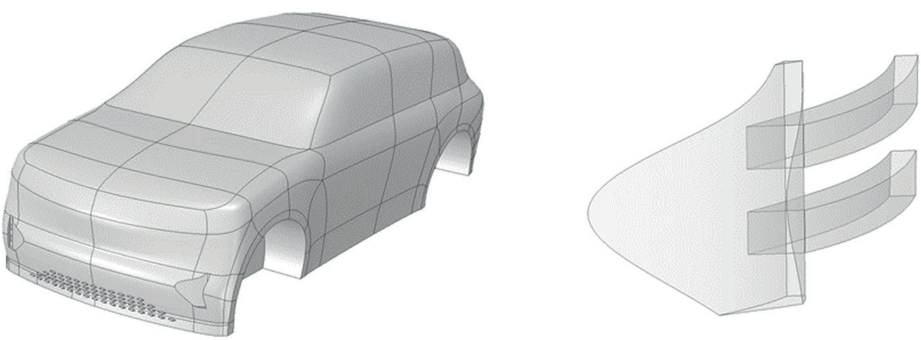

Fig. 8. WT_v3 modification and flow duct details [Created by the authors]

https://doi.org/10.14669/AM/225585

The second group, labelled FRONT, included modifications to the front part of the floor. Three variants, shown in the drawings below, were analysed. This set of solutions was introduced to shape the airflow beneath the car's body and ensure a smooth flow under the floor. The geometries of the FRONT group are shown in the Figures 9–12.

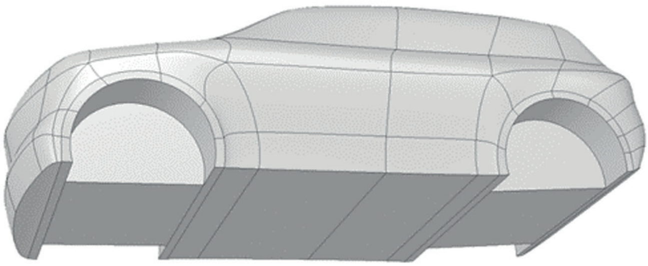

Fig. 9. Base geometry with a view of the floor [Created by the authors]

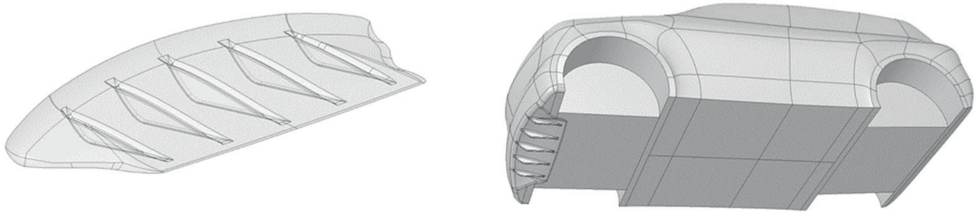

Fig. 10. FRONT_v1 modification and modified floor area [Created by the authors]

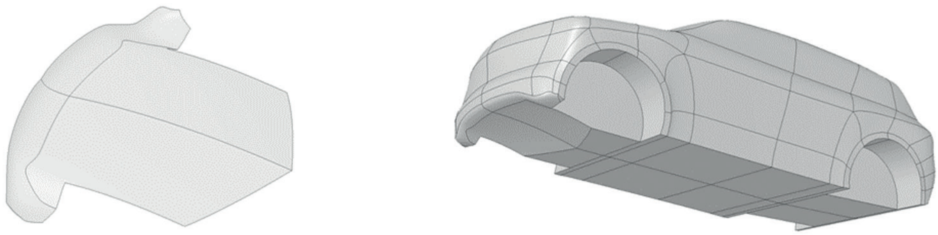

Fig. 11. FRONT_v2 modification and modified floor area [Created by the authors]

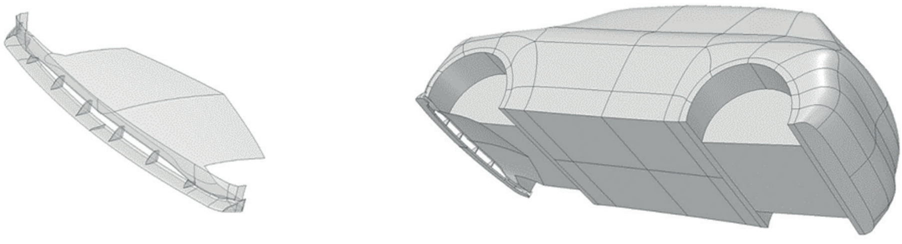

Fig. 12. FRONT_v3 modification and modified floor area [Created by the authors]

https://doi.org/10.14669/AM/225585

The third group, marked REAR, included modifications to the rear part of the floor. It was a combination of a diffuser with flow guides. Three variants presented in the drawings below were analysed. The geometries of the REAR group are shown in the Figures 13–16.

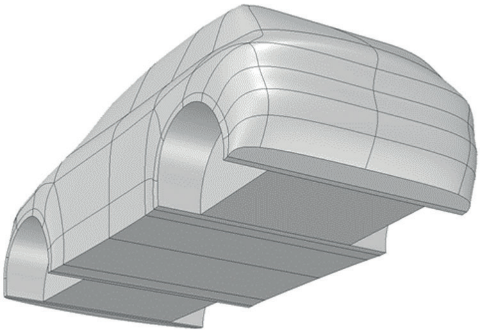

Fig. 13. Base geometry in the rear view [Created by the authors]

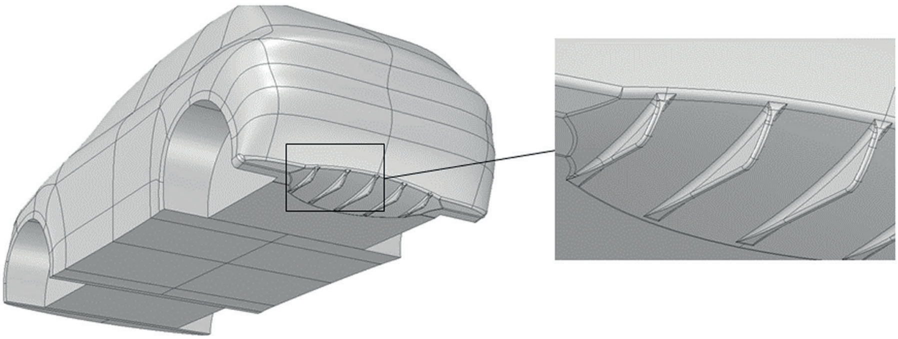

Fig. 14. Modification REAR_v1 and close-up of the modified geometry fragment [Created by the authors]

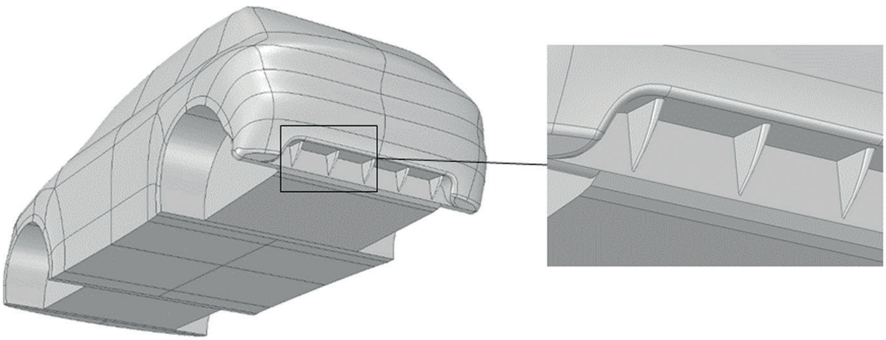

Fig. 15. Modification REAR_v2 and close-up of the modified geometry fragment [Created by the authors]

https://doi.org/10.14669/AM/225585

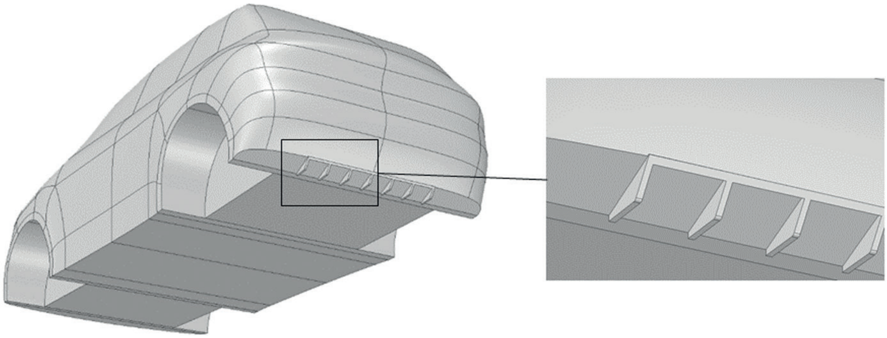

Fig. 16. Modification REAR_v3 and close-up of the modified geometry fragment [Created by the authors]

Numerical calculations were performed using the Ansys Fluent solver [18]. This solver solves Navier-Stokes flow differential equations using the finite volume method (FVM). The RANS (Steady Reynolds-Averaged Navier-Stokes) method was used in the calculations. The k-epsilon turbulence model was adopted. The calculations were performed using second-order discretisation. Due to the low flow velocities, an incompressible and viscous fluid model was used, assuming standard atmospheric conditions at sea level. The model simulated rotating wheels using a moving wall boundary condition and the interaction of the car with the ground using a symmetry boundary condition. The symmetry boundary condition at the ground surface is used interchangeably with the moving wall boundary condition in numerical simulations. In this particular case, it provided greater computational stability than the moving wall boundary condition. This type of modelling is also used in wind tunnels where there is no facility for simulating a moving floor, but it requires the creation of two models.

The symmetry boundary condition, used to simulate the ground effect, is less intuitive than the moving wall condition. However, the author's experience with CFD calculations shows that in similar problems (a car's diffuser, an air intake moving close to the ground), the symmetry boundary condition with a RANS model produced results slightly closer to experimental measurements in terms of pressure distributions on the surfaces of the object under study. Modelling with the moving wall condition tended to underestimate the flow velocity beneath the object. Slightly higher drag forces and lower values of pressure drop were obtained compared to the symmetry condition. RANS numerical analyses using the symmetry model performed well in problems such as shape optimization and comparative analysis of the aerodynamic properties of a given geometry. They allowed for the use of smaller computational grids, accelerated calculations, greater solution stability, which is important for optimization algorithms. It is also worth noting that, despite the use of the symmetry boundary condition to simulate ground effects in the CFD analyses, the computational results still yielded a drag force that was slightly higher than that observed later in the experiment (the drag force reduced by 9.1% in CFD compared to 9.7 % in the experiment). The boundary conditions used are shown in the Figure 17.

https://doi.org/10.14669/AM/225585

The dimensions of the calculation domain were as follows: length 20 m, width 10 m, height 7 m. The computational mesh comprised 18 million of high-quality tetrahedral elements (maximum skewness below 0.8). The mesh had a density scaling factor of 1.1. Y+ factor was in the range from 0.05 to 1.8. The mesh size was selected following a mesh density study to minimise its impact on the results. The convergence criterion was defined as the stabilisation of the monitored drag force and residuals at a level no greater than e–5 for all monitored values. The turbulence intensity at the inlet was set to 0.3% to ensure consistency with wind tunnel tests. The frontal area of the car was 2.479 m².

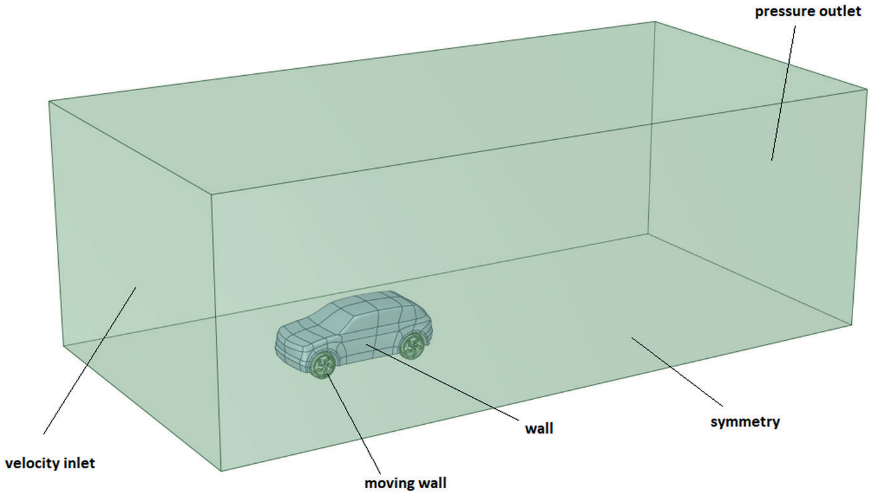

Fig. 17. Computational domain and boundary conditions [Created by the authors]

A computational mesh with tetrahedral elements was used. A view of the surface mesh and selected details is shown in Figure 18.

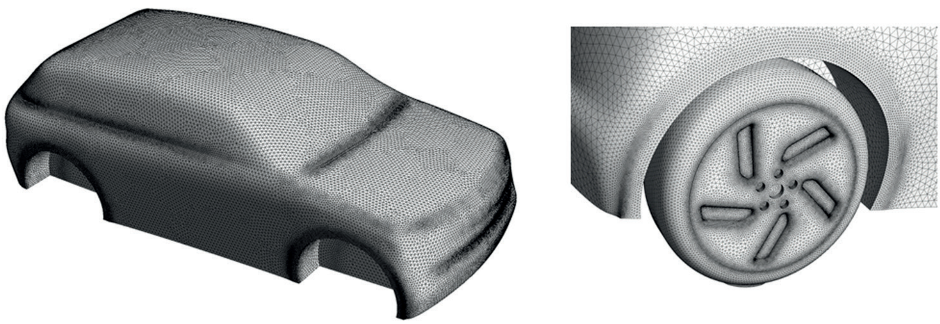

Fig. 18. Surface tetrahedral mesh on vehicle components [Created by the authors]

https://doi.org/10.14669/AM/225585

The Figures 19 and 20 shows colour maps of static pressure on the car body surface and a numerical simulation of limiting streamlines on the body surface for the base geometry at a speed of 120 km/h.

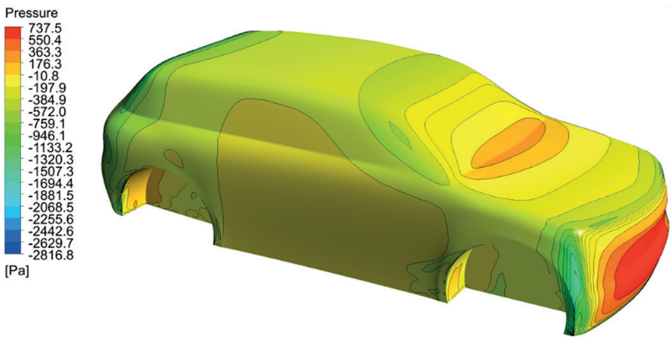

Fig. 19. Static pressure map on the surface of the base body (wheels omitted) for a speed of 120 km/h [Created by the authors]

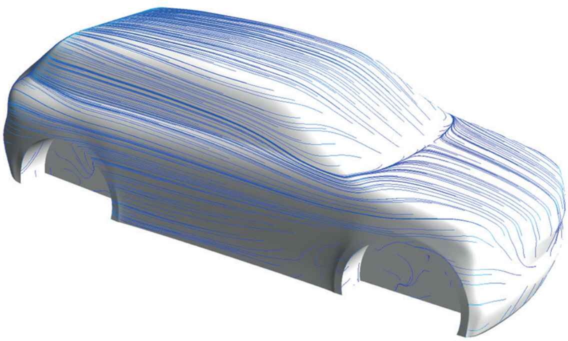

Fig. 20. Limiting streamlines on the body surface (wheels omitted) for a speed of 120 km/h [Created by the authors]

As a result of numerical calculations, the drag force Fx and drag coefficient CD were determined for the base geometry and modified variants. All calculations were performed assuming a constant speed of 120 km/h and no crosswind. Numerical results are presented in Tables 1 and 2.

https://doi.org/10.14669/AM/225585

Tab. 1. Summary of the Fx drag force and CD drag coefficient obtained in CFD calculations for individual configurations and FINAL model which is a compilation of selected solutions

Model	Fx[N]	CD	Change %
BASE	585	0.347	0.0
WT_v1	580	0.344	-0.9
WT_v2	601	0.356	2.7
WT_v3	620	0.368	6.0
FRONT_v1	550	0.326	-6.0
FRONT_v2	570	0.338	-2.6
FRONT_v3	603	0.358	3.1
REAR_v1	611	0.362	4.4
REAR_v2	587	0.348	0.3
REAR_v3	593	0.352	1.4
FINAL	532	0.316	-9.1

The Table 2 presents partial results for vehicle body and wheels. This allows us to analyse the impact of individual solutions on the drag forces generated by the vehicle's wheels.

Tab. 2. Drag force Fx for the car body and wheels and drag coefficient CD for the geometries under consideration and FINAL model which is a compilation of selected solutions

Model	Fx[N]	Fx [N]	Fx [N]	Fx [N]	CD	Change [%]
	car body	front wheels	rear wheels	sum		
BASE	490	49	46	585	0.347	0.0
WT_v1	495	40	45	580	0.344	-0.9
WT_v2	520	39	42	601	0.356	2.7
WT_v3	588	-16	48	620	0.368	6.0
FRONT_v1	436	68	46	550	0.326	-6.0
FRONT_v2	460	59	51	570	0.338	-2.6
FRONT_v3	487	67	49	603	0.358	3.1
REAR_v1	516	51	44	611	0.362	4.4
REAR_v2	490	49	47	587	0.348	0.3
REAR_v3	494	54	46	593	0.352	1.4
FINAL	442	41	49	532	0.316	-9.1

3. Discussion

The study analysed three groups of solutions used in modern passenger cars to reduce the aerodynamic drag of the vehicle body. Each group of solutions was analysed separately, assuming a low degree of mutual interference between them. The results obtained,

https://doi.org/10.14669/AM/225585

presented in Table 1, indicate that the modifications applied to the front of the vehicle, from the FRONT and WT groups, had the greatest effect. The modifications to the rear, from the REAR group, were essentially completely ineffective. However, it should be noted here that these effects may be specific to the adopted base geometry. The rear part of the base geometry already had a correctly shaped diffuser. In addition, the solutions used at the rear are rather strongly related to the flow shaped near the front of the body, and in this case, the initial assumption of no interference with other solutions is questionable.

In the case under study, the proper organisation of the flow in the front part of the floor tested in the FRONT group was of key importance. In practice, this conclusion can be applied mainly in electric vehicles, where this part of the body can be shaped relatively freely. This is much more difficult in combustion engine vehicles, where there is also the issue of air circulation from the radiator and engine area. It is also much more difficult to achieve a completely flat floor in such vehicles, which is important.

When using air ducts blowing air onto the front wheels (WT group), a reduction in front wheels drag was achieved in all cases. The results obtained for the WT_v3 solution are remarkable. While this configuration doesn't reduce drag across the entire vehicle, it does achieve a surprisingly good result in reducing front wheels drag. It can therefore be concluded that solutions of this type, increasingly common in production vehicles, can indeed improve aerodynamics. However, they require proper integration with the overall vehicle geometry.

After analysing the numerical results, it was decided to combine the WT_v1, FRONT_v1 and REAR_v2 solutions in a single body called FINAL. The geometry is shown in Figure 21. Results of numerical calculations of the drag force Fx and drag coefficient CD have been added to the Tables 1 and 2.

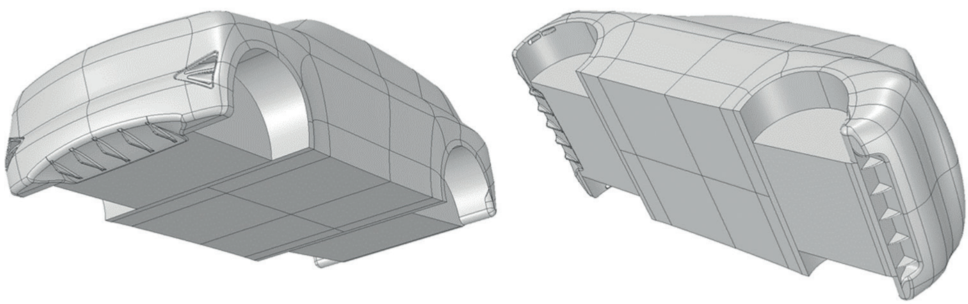

Fig. 21. FRONT_v1, WT_v1, REAR_v2 integrated with BASE model as FINAL geometry [Created by the authors]

https://doi.org/10.14669/AM/225585

Examples of colour maps of static pressure distribution from CFD calculations for selected variants and the base model are shown in Figures 22–24.

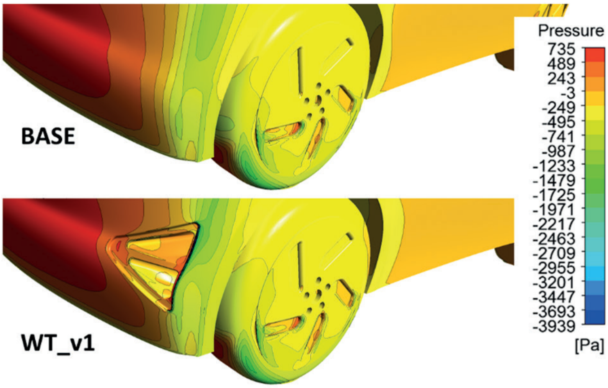

Fig. 22. Pressure colour map comparison for BASE geometry and WT_v1 modification [Created by the authors]

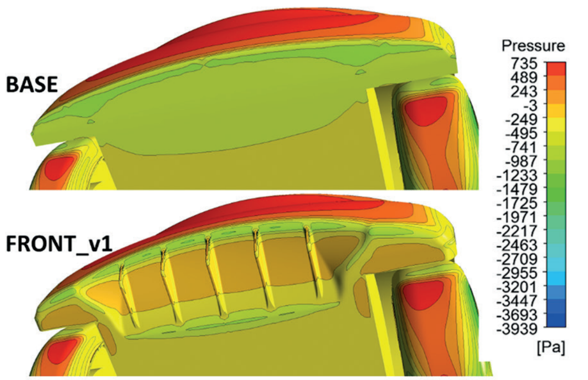

Fig. 23. Pressure colour map comparison for BASE geometry and FRONT_v1 modification [Created by the authors]

https://doi.org/10.14669/AM/225585

Fig. 24. Pressure colour map comparison for BASE geometry and REAR_v2 modification [Created by the authors]

The model prepared in this way was used in comparative experimental wind tunnel tests. The base model on the wind tunnel test stand is shown in Figure 25. Based on wind tunnel tests, conducted by the Łukasiewicz Research Network – Institute of Aviation, it was found that the included modifications reduced the aerodynamic drag by 9.74% compared to the base version.

It should be noted that this result is even slightly better than the partial drag reduction results obtained in the calculations presented in Table 1. Based on the partial results, assuming no interference between the solutions used, it was theoretically possible to reduce drag by approximately 7%. This difference is probably due to strong interference between the flow at the front and rear of the vehicle floor. After improving the flow at the front, the diffuser performance also improved, allowing a better result than the partial results to be achieved.

This may also be the result of discrepancies between the results obtained in CFD and the experimental flow in tunnel conditions. The flow at the rear of the vehicle is particularly difficult to model realistically in numerical terms due to the large separation zone, complex vortex structures and its unsteady, chaotic nature. In addition, there are measurement errors and difficulties in meeting all flow similarity criteria in experimental studies. However, overall, good agreement was found between the CFD and experimental results.

https://doi.org/10.14669/AM/225585

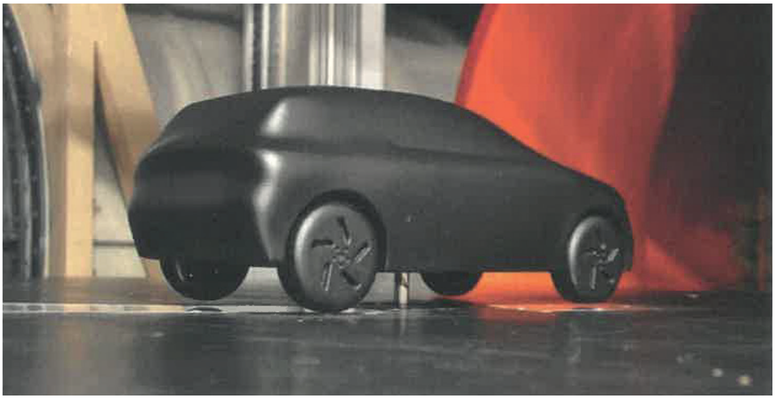

Fig. 25. Base model on the wind tunnel test stand [Created by the authors]

4. Conclusions

- Based on computational and experimental analyses, it can be concluded that additional airflow control elements used locally in the car body can effectively reduce its aerodynamic drag. These solutions can be combined with each other, but interactions may be significant. It should be emphasised, however, that these conclusions were drawn on the basis of a single body geometry under investigation and under specific test conditions. The aerodynamics of a modern car's body are so complex that each solution employed should be tested individually for each vehicle.

- The tested configurations allowed for a total reduction in drag of approximately 9% for tested vehicle geometry and test conditions.

- The best results were achieved by solutions improving the flow under the front part of the vehicle floor. Achieving an orderly flow in this area significantly reduces car body drag.

- Modifications made to the rear of the tested vehicle in test conditions have not proved effective and seem to serve in that simulated car case mainly to increase the visual appeal of the vehicle.

- Using ducts to blow air onto the front wheels is an interesting and effective solution, but it requires careful integration with the entire body shape.

- Additional flow control elements can significantly improve and enhance the visual appeal of the car, increasing the competitiveness of the vehicle both through improved performance and attractive industrial design.

https://doi.org/10.14669/AM/225585

5. Acknowledgement

Most of the work described in this publication was carried out as part of a project financed by the Łukasiewicz Centre.

Grant agreement No. 2/Ł-ILOT/CŁ/2021

PROPEL Optimisation of aerodynamic drag in electric passenger vehicles.

The project was carried out by a consortium consisting of:

Łukasiewicz Research Network – Institute of Aviation,

Łukasiewicz Research Network – Automotive Industry Institute.

6. References

[1] Schuetz T. Aerodynamics of Road Vehicles. 5th edition. SAE International, 2015.

[2] Edgar J. Vehicle aerodynamics: testing, modification & development. Newbury Park (CA), Edgar Media, 2023.

[3] Edgar J. Century of Car Aerodynamics: the Science and Art of Cars and Airflow. Amazon Digital Services LLC, 2021.

[4] Fabian M, Hunady R, Kupec F, Mlaka T. Effect of the Aerodynamic Elements of the Hatch-back Tailgate on the Aerodynamic Drag of the Vehicle. Advances in Science and Technology Research Journal. 2022;16(6):73–87. https://doi.org/10.12913/22998624/155308.

[5] Li J, Zhu X, Zhang C, Dang S, Chen G. CFD simulation of passenger car aerodynamics and body parameter optimization. Fluid Dynamics and Materials Processing. 2025;21(9):2305–2329. https://doi.org/10.32604/fdmp.2025.067087.

[6] Kurec K, Piechna J. Influence of Side Spoilers on the Aerodynamic Properties of a Sports Car. Energies. 2019;12(24):4697. https://doi.org/10.3390/en12244697.

[7] Abbas MK, Aldabash NM, Almahdawi YAJ, Azzawi IDJ, Al-Obaidi MA. Synergistic experimental-numerical study for assessing the aerodynamic performance of a simplified road vehicle. Advances in Science and Technology Research Journal. 2026;20(5):322–334. https://doi.org/10.12913/22998624/215653.

[8] Peter B, Lakatos I. Comparison of Different Turbulence Models and Wall Treatment Methods for Vehicle Aerodynamics Investigations. Periodica Polytechnica Transportation Engineering. 2024;52(1):67–74. https://doi.org/10.3311/PPtr.22671.

[9] Şumnu A, Eraslan Y. Aerodynamic shape optimization of simplified ground vehicle (Ahmed body) using passive control devices. Mechanika. 2025;31(1). https://doi.org/10.5755/j02.mech.36452.

[10] Kuttasirisuk N, Munikanon P, Ajavakom N, De Silva P, Phanomchoeng G. Simulation-guided aerodynamic design and scaled verification for high-performance sports cars. Modelling. 2025;6(3):105. https://doi.org/10.3390/modelling6030105.

[11] Chowdhury H, Bavin Loganathan B, Mustarya I, Moriab H, Alam F. Effect of various deflectors on drag reduction for trucks. Energy Procedia. 2017;110:561–566. https://doi.org/10.1016/j.egypro.2017.03.185.

[12] Wang J, Li H, Liu Y, Liu T, Gao H. Aerodynamic research of a racing car based on wind tunnel test and computational fluid dynamics. MATEC Web of Conferences. 2018;153(7):04011. https://doi.org/10.1051/matecconf/201815304011.

[13] Singh P, Gupta H, Vinayak O, Tyagi A. Application of Response Surface Method and Genetic Algorithm in the Design of High-Efficiency Prototype Vehicle. 14th Asian Computational Fluid Dynamics Conference. 2023;arXiv:2311.04308. https://doi.org/10.48550/arXiv.2311.04308.

https://doi.org/10.14669/AM/225585

[14] Buil RM, Angulo DR, Baquedano JAP. Experimental full scale tests on vortex generators for heavy vehicles drag reduction. DYNA. 2018;93(1):96–101. https://doi.org/10.6036/8321.

[15] Islam RA, Hossain A, Mashud I, Gias TI. Drag Reduction of a Car by Using Vortex Generator. International Journal of Scientific and Engineering Research. 2013;4(7):1298–1302. https://www.researchgate.net/publication/340953419_Drag_Reduction_of_a_Car_by_Using_Vortex_Generator (accessed on 25.06. 2026).

[16] Izera SUV – images. OtoEV.pl: https://otoev.pl/modele-ev/izera/izera_suv (accessed on 25.06.2026).

[17] Volkswagen ID.4 – images. Volkswagen Newsroom: https://www.volkswagen-newsroom.com/en/images/albums/id-4-6723 (accessed on 25.06. 2026).

[18] Ansys Fluent Fluid Simulation Software. 2025: https://www.ansys.com/products/fluids/ansys-fluent (accessed on 10.12.2025).